RSC Advances

PAPER

View Article Online
View Journal | View Issue

Cite this: *RSC Adv.*, 2022, **12**, 32994

Metallic boro-carbides of A_2BC (A = Ti, Zr, Hf and W): a comprehensive theoretical study for thermo-mechanical and optoelectronic applications†

R. Islam,[ab] M. M. Hossain, *[ab] M. A. Ali, [ab] M. M. Uddin[ab] and S. H. Naqib [bc]

High-hardness materials with ductile deformation behavior have recently piqued interest due to their prospective applications, particularly as hard and protective coatings. The crack formation, especially in metal and ceramic materials, is one of the biggest problems of the surface hard coatings on heavy-duty tools. In this regard, mechanical properties (Vickers hardness, fracture toughness, machinability index, index of brittleness, as well as Pugh's ratio) have been studied for the metallic boro-carbides of A_2BC (A = Ti, Zr, Hf, and W) compounds using the state-of-the-art density functional theory in detail. The compounds under investigation are both thermodynamically and mechanically stable. The value of Vickers hardness (in GPa) for A_2BC (A = Ti, Zr, Hf, and W) compounds are 28.20, 23.12, 12.44, and 35.70, respectively, which indicates the W_2BC could be a member of the hard family (H_v > 30 GPa). Pugh's ratio suggests ductile deformation for the W_2BC compound, whereas the other three (Ti_2BC, Zr_2BC, and Hf_2BC) compounds exhibit brittle deformation behavior. The W_2BC compounds have the highest ductility among the other metallic boro-carbides (M_2BC; M = V, Nb, Mo and Ta) and some other benchmark coating materials (TiN, TiAlN, C-BN, and $Cr_{0.5}Al_{0.5}N$). The fracture toughness (K_{IC}) values are in the following sequence: Zr_2BC < Ti_2BC < Hf_2BC < W_2BC, which indicates that, the highest resistance (K_{IC} = 4.96 $MPam^{1/2}$) found for W_2BC is suitable to prevent the crack propagation within the solid. In addition, the structural, electronic, optical, and thermal properties are also investigated for the A_2BC (A = Ti, Zr, Hf, and W) compounds. The Ti_2BC (W_2BC) reflectivity spectra never fall below 53 (45)% in the 0 to 10.3 eV (0 to 16.70 eV) photon energy range, suggesting that these compounds have promise for usage as coating materials to reduce solar heating. Hf_2BC and W_2BC compounds could also be exploited as promising thermal barrier coating materials, while Ti_2BC could be used as heat sink material based on the results of Debye temperature, melting temperature, thermal conductivity, and thermal expansion coefficient. The electronic properties reveal the metallic behavior of these compounds. The results obtained here are compared with those of some commercially known compounds, where available.

Received 30th August 2022
Accepted 11th November 2022

DOI: 10.1039/d2ra05448e

rsc.li/rsc-advances

1. Introduction

Despite the numerous benefits of ceramic materials (for example, TiN, TiAlN, c-BN, $Ti_{0.5}Al_{0.5}N$, $Ti_{0.25}Al_{0.75}N$, $Cr_{0.5}Al_{0.5}N$ *etc.*) such as high chemical stability, higher mechanical characteristics and hardness, stiffness, oxidation and corrosion resistance, the usage of these materials as surface hard coatings on cutting tools and other heavy-duty tools in abrasive applications is limited.[1–7]One of the most serious issues is the formation of cracks in the material's surface, which greatly reduces the tool's lifetime and, as a result, its performance.[3] Many researchers, industrialists and investors are working hard to find a solution to this significant problem. The main problem is the brittle characteristics and can be solved by increasing their ductility index *via* materials engineering. There are two main approaches for increasing ductility: (1) nanostructuring and (2) finding novel materials with high stiffness and innately ductile/damage tolerant properties.[3] Pugh proposed that a material's inherent ductility is determined by the shear to bulk modulus ratio being less than a critical value 0.57.[8]

The nanostructure of the Mo_2BC compound was grown using magnetron sputtering technique and nanoindentation was used to investigate the mechanical features such as stiffness and level of ductility.[4] The Mo_2BC has an orthorhombic structure with a space group *Cmcm*. A combination of boride and carbide subcells make up the crystal structure of Mo_2BC. The boron-formed curving chain is positioned in the Mo_6B trigonal

[a]*Department of Physics, Chittagong University of Engineering and Technology (CUET), Chattogram-4349, Bangladesh. E-mail: mukter_phy@cuet.ac.bd*

[b]*Advanced Computational Materials Research Laboratory, Department of Physics, Chittagong University of Engineering and Technology (CUET), Chattogram-4349, Bangladesh*

[c]*Department of Physics, University of Rajshahi, Rajshahi 6205, Bangladesh*

† Electronic supplementary information (ESI) available. See DOI: https://doi.org/10.1039/d2ra05448e

prism, while the C atoms are located at the octahedral positions in the Mo_6C prism.[9,10] The experimentally measured Young's modulus and hardness value of Mo_2BC was 460 GPa and 29 ± 2 GPa, respectively.[4] The bulk modulus value of 324 GPa, which expresses the stiffness of a material, is higher than that of commercially available compounds such as TiN (295 GPa) and $Ti_{0.25}Al_{0.75}N$ (178 GPa) but lower than c-BN (376 GPa).[3,4]

The Mo_2BC crystal with dimensions 10 mm in length and 3 mm in diameter was grown using the Czochralski method.[10,11] P. Lejay *et al.*[10] investigated the effect of metal substitution into $Mo_{2-x}M_xBC$ (M = Zr, Nb, Rh, Hf, Ta, W) compound and found its superconducting (Type-II) behavior with critical temperature above $T_c = 4.2$ K. It was envisaged that replacing the Mo atom in the Mo_2BC compound with some transition metals could improved physical properties at some specific sectors. The structural, mechanical, and electronic band structures of X_2BC (X= Mo, Ti, V, Zr, Nb, Hf, Ta, and W) were investigated by Bolvardi *et al.*[3] They reported that all the compounds are mechanically and thermodynamically stable. Also, X_2BC (X= Ta, Mo and W) compounds showed high stiffness and moderate ductility, indicating the application as cutting and forming tools. Specifically, the bulk modulus of W_2BC is 350 GPa, which is 93% of the value of commercialized compounds, c-BN. P. Barua *et al.*[1] reported a comprehensive study of structural, mechanical, hardness, electronic, thermal and optical properties of M_2BC (M = V, Nb, Mo and Ta) compounds. These compounds show excellent thermal and optical properties that could be helpful in the design of thermo-mechanical and optoelectronic devices. For the usage as thermal barrier coating (TBC) material, researchers are looking for the materials with high hardness and malleable in nature. At present, some materials such as c-BN, TiN, TiAlN, $Ti_{0.25}Al_{0.75}N$, $Ti_{0.5}Al_{0.5}N$ and $Cr_{0.5}Al_{0.5}N$ are used as hard coating materials but their brittleness is prominent.[2–5,12] To partially address this problem and the reported excellent thermal and optical properties in compounds of a similar type such as M_2BC (M = V, Nb, Mo and Ta),[1] we are strongly motivated to study the physical properties of A_2BC (A = Ti, Zr, Hf, and W) compounds. Various vital physical features, such as mechanical (Vickers hardness, fracture toughness, index of brittleness, machinability index) and electronic (band profile, Fermi surface, charge density, Mulliken population analysis) properties of metallic boro-carbides of A_2BC (A = Ti, Zr, Hf, and W) compounds are still unexplored from the standpoint of device applications in many areas. Some thermal properties such as Debye temperature, minimum thermal conductivity, Grüneisen parameter, thermal expansion coefficient, specific heat of these compounds are entirely unexplored. Knowledge on these thermophysical properties are prerequisites to any possible thermal device application. Furthermore, numerous optical features that are technologically essential (dielectric function, refractive index, absorption coefficient, photoconductivity, reflectivity, and loss function) have not been adequately researched till date.

Therefore, in the present study, a detailed investigation of structural, electronic, mechanical, optical and thermal properties of A_2BC (A = Ti, Zr, Hf, and W) compounds will be reported to understand the physical states of these compounds further. We will also go over some mechanical and electronic parameters again to double-check the accuracy of our findings and provide some extra information. The obtained results suggested that Ti_2BC and W_2BC compounds have notable promise as coating materials to reduce solar heating. Also, Hf_2BC and W_2BC compounds can be exploited as promising thermal barrier coating materials.

2. Theoretical methodologies

The first-principles technique was used to explore metallic boro-carbides of A_2BC (A = Ti, Zr, Hf, and W) compounds utilizing the state-of-the-art density functional theory.[13] The high-throughput calculations are done in the CAmbridge Serial Total Energy Package (CASTEP)[14,15] platform. The generalized gradient approximation (GGA) is used for electron exchange correlation function with the Perdew–Burke–Ernzerhof (PBE) functional.[16] The obtained results in this study are based on ultrasoft pseudopotential.[1] The cut-off energy is taken to be 500 eV for all the compounds for the plane wave expansion process. Broyden–Fletcher–Goldfarb–Shanno (BFGS) approach has been adopted for atomic configuration optimization. During the optimization process the following additional parameters are used: *k*-point sampling of 8 × 2 × 8 special points in a Monkhorst–pack grid;[17] energy convergence thresholds of 5×10^{-6} eV atom^{-1}; maximum force of 0.01 eV Å^{-1}; maximum stress of 0.02 GPa and maximum displacement of 5×10^{-4} Å. The single crystal stiffness constants, C_{ij}, are calculated using the 'stress–strain' approach enabled in the CASTEP code.[14] These stiffness constants are then used to obtain the bulk modulus, *B*, Young modulus, *Y*, and shear modulus, *G*. The theory of optical properties and relevant formulae can be found in prior reports.[18,19] The analysis of Mulliken population is used to calculate the value of Vickers hardness ($H\nu$) of all the compounds under study.

3. Results and discussion

3.1 Structural properties

The metallic boro-carbides of A_2BC (A = Ti, Zr, Hf, and W) belong to orthorhombic crystal system with space group: *Cmcm* (#No.:61).[1,3,4] The optimized crystal structure of Ti_2BC, as an example, is shown in Fig. S1.† This orthorhombic unit cell contains 16 atoms in total, in which 8 atoms are A-element and each of B and C contains 4 atoms. The stability of the compounds under study was ensured by the calculation of the formation enthalpy which has been reported in ref. 3. The crystal structure (conventional unit cell) is first optimized and then the ground state lattice parameters and volume of the unit cell are obtained. It is noticed that the changes of *b*-axis lattice parameter for all compounds are significantly increased compared to *a*- and *c*-axis when we go from Ti to Zr to Hf. The calculated lattice parameters are well matched with previous report as the variation is less than 1%.[3] The value of lattice parameters and volumes of the A_2BC (A = Ti, Zr, Hf, and W) compounds are given in Table S1.†

3.2 Electronic properties, charge density and Fermi surface

The electronic band structure (BS) are calculated along the high symmetry directions following the paths G-Z-T-Y-S-X-U-R within the Brillouin zone (BZ) and electronic energy density of states (DOS) over the whole BZ of A_2BC (A = Ti, Zr, Hf, and W) compounds as shown in Fig. 1(a–d) and Fig. S2(a–d).† These band structure features are closely linked to charge density, atomic bonding and Fermi surface topology. The Fermi level (E_F) is denoted by the horizontal dashed line and set at 0 eV. The valence bands (VB) are clearly crossing the E_F which is a signature of the metallic behavior of the systems. The total density of states (TDOS) describes the gross contribution to the electronic transport properties while the partial density of states (PDOS) elucidates the individual atomic contribution to the same. The TDOS value of A_2BC (A = Ti, Zr, Hf, and W) compounds are 5.80, 5.85, 4.76 and 5.41 states per eV, respectively. It is seen from the BS that the band dispersion along the path Y–S at E_F is strongly non-dispersive compared to any other symmetry path in all the studied compounds. This non-dispersive nature could account for a high DOS value. It is noticed that the highest contribution to the TDOS for A_2BC (A = Ti, Zr, Hf, and W) comes from the d-orbital electrons of Ti, Zr, Hf and W elements. The DOS spectrum of VB can be divided into two sub-bands, ranging from −15 to −7.5 eV and (−7.5 to 0) eV, based on its composition. It is observed that the formation of total band in the energy range of −15 to −7.5 eV for all title compounds is mainly comprised of the hybridization of C-2p, B-2s and B-2p orbitals. Again, in the range of (−7.5 to 0) eV, the band is formed by the hybridization of C-2p, B-2p and W-5d electronic states. The contribution of 6s and 5p orbitals of the elements Ti/Zr/Hf/W to the composition of the energy bands is minimal.

The Fig. 2 depicts the electron density difference (EDD) for A_2BC (A = Ti, Zr, Hf, and W) compounds, as well as the adjacent scale bar (+0.1 to −0.1). It has been found that all of the compounds under study have an asymmetric charge distribution at various atomic species. The red hue in the mapping images represents the level of charge accumulation, whereas the blue color represents charge depletion. It is seen that the electron is transferred from A element (Ti, Zr, Hf and W) to B/C element, which is an indication of ionic bonding. On the other hand, the strong covalent bond (due to the accumulation of charge) between the Ti/Zr/Hf/W–B/C is found. It is noted here that the covalent bond between Ti/Zr/Hf/W–C is much stronger than the Ti/Zr/Hf/W–B bond. The charge accumulation at B species was gradually decreased, while the charge depletion at

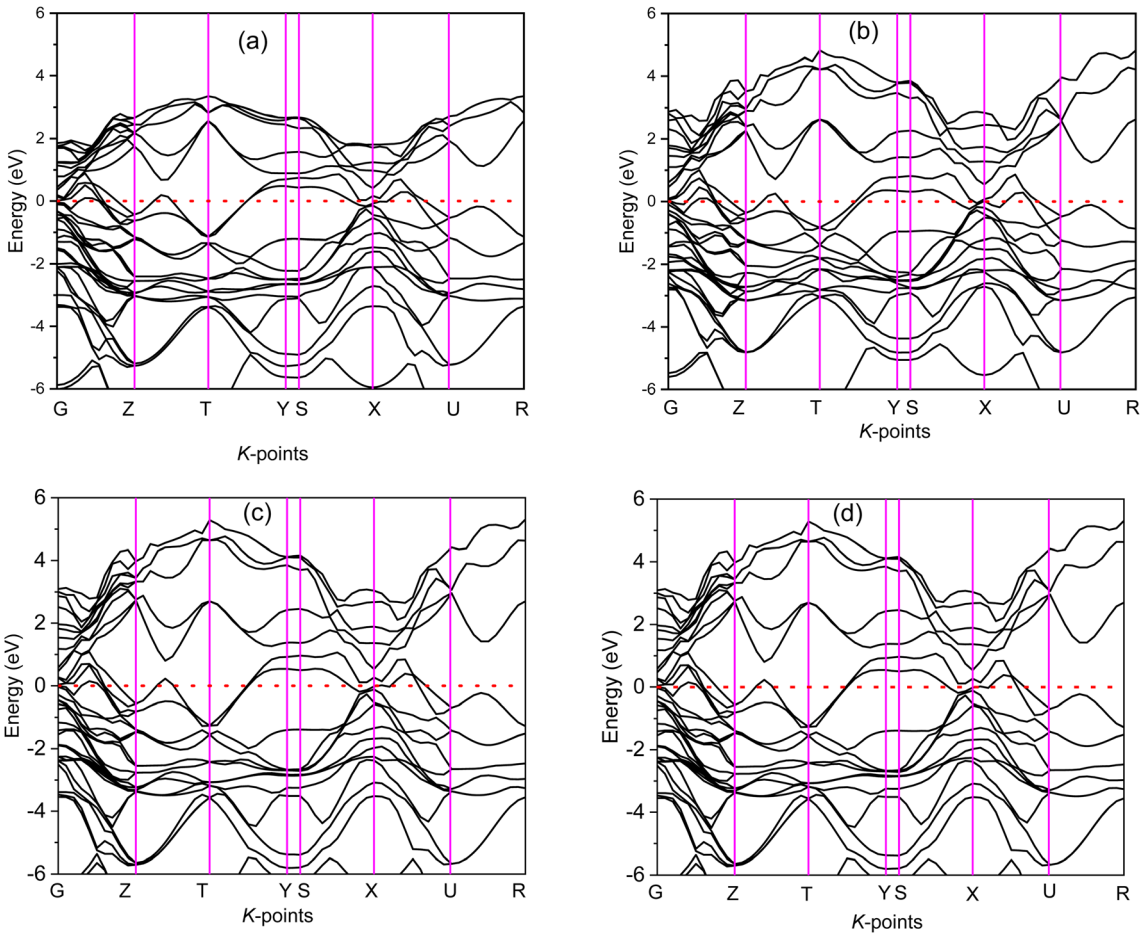

Fig. 1 The electronic band structure calculated along high symmetry directions following the paths G-Z-T-Y-S-X-U-R within the Brillouin zone for (a) Ti_2BC, (b) Zr_2BC, (c) Hf_2BC and (d) W_2BC compounds.

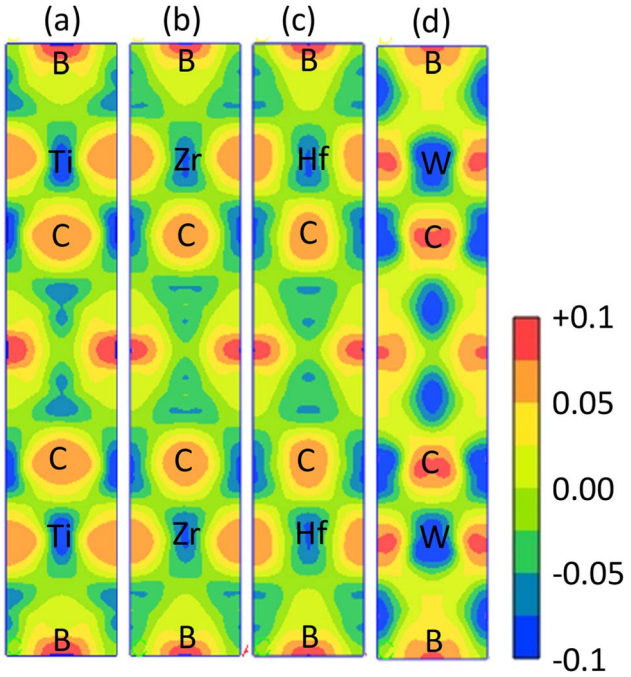

Fig. 2 Mapping images of electron density difference for (a) Ti_2BC, (b) Zr_2BC, (c) Hf_2BC and (d) W_2BC compounds. The adjacent scale bar is showing the values of charge in the range from −0.1 to +0.1 (electronic charge).

metallic A species was gradually increased in the order of W_2BC > Ti_2BC > Zr_2BC > Hf_2BC compounds and accordingly, the bond strength. The non-directional metallic bonding between transition metal A elements can also be found. In summary, the mixture of bonding (ionic, covalent and metallic bond) characteristics has been found in the all the compounds under investigation.

The Fermi surfaces of metals are useful for characterizing and predicting the thermal, electrical as well as optical properties. In Fig. 3, the Fermi surfaces of A_2BC (A = Ti, Zr, Hf, and W) compounds are shown. Depending on the composition, the Fermi surface features differ in shape and position. Therefore, it implies that electrons motion on the Fermi surface and accordingly, charge transport properties will be different for the A_2BC (A = Ti, Zr, Hf, and W) compounds. The Fermi surface structure of the W_2BC compound is completely different from that of the other (Zr_2BC, Hf_2BC, and W_2BC) compounds. In the G-X direction, a cylinder with an octahedral shape can be found as hole pocket. Additionally, five similar-shaped sheets are oriented in the same direction. The Ti_2BC and Hf_2BC compounds have nearly identical Fermi surfaces. In both these compounds, a rectangle-shaped cylinder is observed along the G-X direction, which can be considered as hole pocket. Furthermore, there are two almost similarly shaped cylinders on either side of it along the G-Z directions. Along the G-Z direction, there are additionally three curvy sheets. The open surfaces positioned in the Y–S direction at the edge of BZ are considered as electron pockets, as shown for the Ti_2BC, Zr_2BC and Hf_2BC compounds. The Fermi surface of Zr_2BC is almost similar to those of Ti_2BC and Hf_2BC, the only exception being that an octahedral cylinder can be found along the G-X direction.

3.3 Optical properties

Before delving into the optical functions, it is necessary to understand the frequency/energy dependent dielectric function (real and imaginary parts). The optical functions of any homogeneous medium at all photon energies can be described by the dielectric function. The imaginary part of the dielectric function (IDF) is directly related to the electronic band structure and is calculated from the momentum matrix element through a possible electronic transition between two electronic states in the Brillouin zone from the valence band to the conduction band. The real part of the dielectric function (RDF) can be obtained using the Kramers–Kronig relations.[15,18] Once an IDF(ε_2)

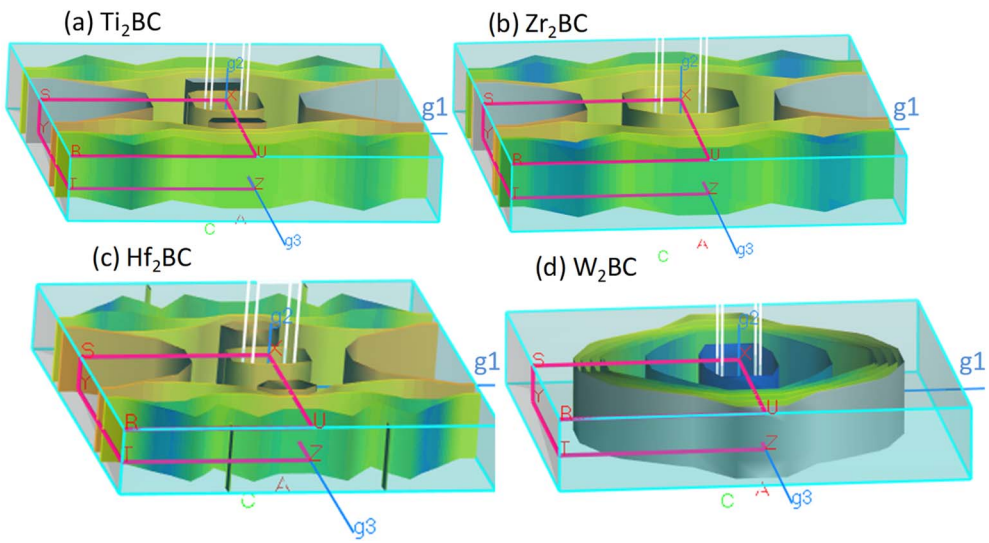

Fig. 3 The Fermi surface of the metallic boro-carbides of (a) Ti_2BC, (b) Zr_2BC, (c) Hf_2BC and (d) W_2BC compounds.

and an RDF(ε_1) are obtained, all the other optical functions such as photoconductivity, absorption coefficient, refractive index, reflectivity, and loss function can be derived. The details of the theory and the relevant formulae can be found in the literature.[14,15,18,19]

The RDF(ε_1) and IDF(ε_2) of A_2BC (A = Ti, Zr, Hf, and W) compounds are illustrated in Fig. S3(a).† The IDFs for all the compounds are gradually reduced from a positive value as the incident photon energy increases. This is a very common occurrence in metallic systems. However, in the range of 7.0–9.0 eV photon energies, the IDF (ε_2) values for all the compounds were zero. The RDF (ε_1) spectra for all examined compounds, on the other hand, shows prominent peaks at roughly 1 eV and thereafter goes zero from negative value in the energy range of 9.0–12.0 eV. Both the spectra (RDF and IDF) ensure the Drude like behavior of the compounds.

The refractive index (n) compares the velocity of light in any medium with that in empty space, whereas the extinction coefficient (k) indicates how much light is absorbed by the material. Fig. S3(b)† displays the refractive index (n) and the extinction coefficient (k) for all the compounds under consideration. It is seen that for A_2BC (A = Ti, Zr, Hf, and W) compounds, the values of n at zero photon energy/frequency are 20.68, 8.96, 12.12, and 15.95, respectively. For enhancing the visual features of electronic displays, high refractive index materials (typically larger than 1.50) are beneficial in photonic and optoelectronic device applications such as LCDs, OLEDs, and QDLED televisions.[18,20,21] Furthermore, materials having a high refractive index are frequently combined with materials with a low refractive index to create transparent components with enhanced anti-reflective qualities.[22] It is noted here that, among all the compounds, the highest refractive index (20.68) is found for Ti_2BC and the lowest (8.96) for the Zr_2BC compound. The spectrum of k shows that the sequence of maximum low-energy light absorption in the studied materials is as follows: $Ti_2BC > W_2BC > Hf_2BC > Zr_2BC$, since the highest peak for each studied compound was obtained at about 1 eV photon energy.

The spectrum of the absorption coefficient (α) of A_2BC (A = Ti, Zr, Hf and W) is shown in Fig. 4(a). It can be seen that absorption starts from the zero photon energy. This behavior is a signature of the metallic nature of these compounds, which was also confirmed by the investigations of the electronic band structures. However, the value of the absorption coefficient increases with the incident photon energy. The highest values of α of 2.15 $\times 10^5$, 2.03 $\times 10^5$ and 3.0 $\times 10^5$ (all units are cm^{-1}) at 5.80 eV, 6.80 eV and 6.40 eV for A_2BC (A = Ti, Zr and W) compounds are found, while for the Hf_2BC compound, a significantly lower absorption occurs with the value of $\alpha = 0.8 \times 10^5$ cm^{-1} at photon energy of 6.0 eV. The possible reason can be explained from the TDOS value in Fig. S2.† The TDOS value of the Hf_2BC compound at the Fermi level is the lowest among all the compounds under study. The lower the available electronic states, the lower the possibility of photon absorption.

Optical conductivity also begins when low-energy electromagnetic radiation (photon energy) is just incident on the material (Fig. 4(b)), further verifying the metallic character. The photoconductivity increases sharply in the IR region and then gradually decreases with several notable peaks. The positions of these peaks are determined by the peaks in the electronic energy density of states. The photoconductivity spectrum of the W_2BC compound, for example, has peaks at 0.85, 2.9, and 6.33 eV photon energies, and then drops to zero at 16 eV. However, a significant photoconductivity could be found at least for a wide range of photon energies from 0 to 10 eV. The rest of the compounds under study show qualitatively similar character.

The reflectivity spectra start at 80%, 60%, 70% and 75% for A_2BC (A = Ti, Zr, Hf and W) compounds, respectively, as shown in Fig. 5(a). It is also noted that the Ti_2BC (W_2BC) reflectivity spectra never fall below 53 (45)% in the 0 to 10.3 eV (0 to 16.70 eV) photon energy range, while the spectra for Zr_2BC and Hf_2BC compounds drop below 40%. Furthermore, the maximum reflectivity for all studied compounds can be found in the UV range within photon energy of 7.5–11.2 eV. The spectra for Ti_2BC and W_2BC never go below 53% up to 5 eV. This means that 53% or more photons are reflected in the IR, visible and UV (from 3.1 to 5 eV). The value of reflectivity spectra of these two compounds (Ti_2BC and W_2BC) are much higher than that of other metallic boro-carbides of M_2BC (M = V, Nb, Mo and Ta),[1] $TmCu_3S_4$ (Tm = V, Ta, Nb),[23] $La_2Q_2O_7$ (Q = Ge, Sn),[24] some 211

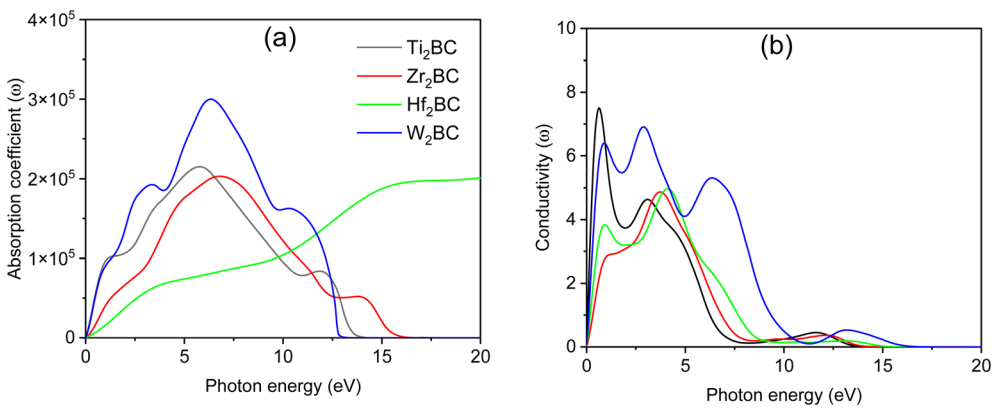

Fig. 4 (a) Absorption coefficient and (b) photoconductivity *versus* photon energy of the A_2BC (A = Ti, Zr, Hf, and W) compounds.

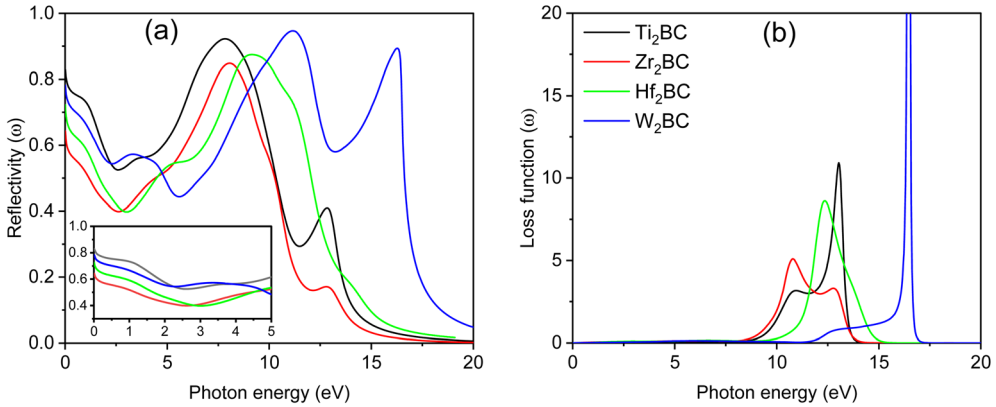

Fig. 5 (a) Reflectivity and (b) loss function *versus* photon energy of the A_2BC (A = Ti, Zr, Hf, and W) compounds. The inset shows the reflectivity spectra in the visible and near-UV range (up to 5 eV).

MAX phase compounds[25–28] and others[29] in the energy region of 0–6 eV. According to prior research, a material with a reflectivity of at least about 44% may be able to avoid solar heating.[1,27,30,31] The excellent reflectivity properties of Ti_2BC and W_2BC, in particular, show promise in coating technology designed to avoid solar heating.

The loss function, $L(\omega)$, quantifies the energy lost by charged particles such as electrons passing through a material. It is seen from Fig. 5(b) that there is no loss of energy up to 0–8.55 eV for all the compounds under study due to the comparatively large value of $[\varepsilon_2(\omega)]$. Maximum energy loss is noticed when a plasma resonance occurs. Prominent peaks (expressing the energy loss of the charged particle) for A_2BC (A = Ti, Zr, Hf and W) are found at 13, 10.77, 12.35 and 16.50 eV, respectively. At these particular energies the reflection and absorption spectra exhibit drastic falls and the compounds under investigation are expected to show high transmittance.

3.4 Mechanical properties

3.4.1 Elastic stiffness constant and elastic moduli. In order to explain the mechanical behavior of materials, the elastic constants of single crystals must first be investigated. The value of the stiffness constant can demonstrate the bond strength in a particular direction. One of the important factors for studying a material's mechanical properties is its mechanical stability. The criteria for mechanical stability of an unstressed crystalline system are determined by the inequality of elastic constants. The stability conditions for orthorhombic system are expressed *via* the following inequalities:[32,33]

$$C_{11} > 0;\ C_{44} > 0;\ C_{55} > 0;\ C_{66} > 0;$$

$$C_{11}C_{22} > C_{12}2;\ (C_{11}C_{22}C_{33} + 2C_{12}C_{13}C_{23}) > (C_{11}C_{23}2 + C_{22}C_{13}2 + C_{33}C_{12}2)$$

As can be seen from Table S2,† the above-mentioned conditions are satisfied by the calculated elastic constants for all the compounds under study. Therefore, the A_2BC (A = Ti, Zr, Hf, and W) compounds can be said to be mechanically stable. In addition to the confirmation of mechanical stability, some interesting features can also be evaluated from elastic stiffness constant, C_{ij}. In the present study, all the compounds have $C_{33} > C_{11}$, implying that atomic bonding should be stronger along the *c*-axis than that along the *a*-axis. The values of C_{11} and C_{33} are much higher than C_{44}. This indicates that the linear elastic strain along the [100] and [001] directions is much harder to produce than the shear strain of all the compounds under study. It is also noticeable from Table S2† that the value of the elastic stiffness coefficient C_{66} is higher than C_{44} for all the compounds. This reflects that the ability to resist deformation for basal plane and prismatic slip shear along the [110] direction should be higher than that along the [010] direction in the (100) plane. According to previous report,[34] the shear constant C_{44} is one of the best predictors of a material's hardness. Therefore, as seen in the Table S2,† the W_2BC compound should have the highest hardness among all the investigated compounds, as its C_{44} value is the highest.

The Cauchy pressure (CP) explains which type of chemical bond dominates in a compound. The value of CP is determined by the following relation: $CP = C_{12} - C_{44}$. The positive sign of CP indicates dominance of ionic bonding, while the negative sign means a dominance of covalent bonding in the material.[1,33,35] From the present study (Table S2†), it is worth noting that the covalent bond dominates in the Ti_2BC compound, while the ionic bond is dominating in the W_2BC. The other two compounds exhibit a good balance of covalent/ionic bonding within the crystals.

The modulus of elasticity for an elastic material is usually assessed as the bond strength among atoms in a solid. The three types of elastic moduli (bulk modulus (B), shear modulus (G), and Young's modulus (Y)) can be computed from the single crystal elastic constants utilizing the Voigt–Reuss–Hill (VRH) approximation.[36,37] These moduli mainly reveal the mechanical behavior of solids under stress and reflect the capability of materials to resist elastic deformations of various types. The associated formulas and theories can be found in previous literatures.[1,18,21,33] The results of calculations of the moduli of

elasticity for A_2BC (A = Ti, Zr, Hf, and W) compounds are given in Table 1. It is seen from Table 1 that the highest value of elastic moduli ($B = 353$, $G = 188$ and $Y = 479$; all are in GPa) is found for the W_2BC compound, which should show the highest resistance to elastic deformation compared to other studied compounds. It is instructive to compare the elastic constants of W_2BC with a well-known commercial compound, TiAlN, that is normally used as a surface hard coating on various tools. The values of B, G and Y for W_2BC are higher by 27.20%, 5.30% and 9.40% from those of TiAlN,[2,5] and higher by 49.57%, 34.57% and 37.36% from those of $Ti_{0.25}Al_{0.75}N$.[4] Also those values are higher by 29.17%, 20.21% and 21.71% from $Cr_{0.5}Al_{0.5}N$.[7] However, these elastic moduli of W_2BC are much lower than those of commercialized compound c-BN. It should be noted here that the B value, which expresses the resistance to volume deformation, is only 6.50% lower than that of the c-BN compound.[4]

The malleability/brittleness of a solid can be predicted by Poisson's ratio (ν) and Pugh ratio (G/B). A value $G/B > 0.571$ and $\nu < 0.26$, is an indication of brittleness, otherwise implies malleability of solid.[8,18,21,27,35] In this study, it is seen from Table 1 that the W_2BC compound meets the criteria ($G/B = 0.53$) for malleability or ductility behavior, while the other three compounds (Ti_2BC, Zr_2BC and Hf_2BC) show brittle behavior. Interestingly, the W_2BC compounds have the highest ductility among all the metallic boro-carbides (X_2BC; X= Mo, Ti, V, Zr, Nb, Hf, Ta, and W). The hardness of this compound is also the highest. It should be noted that the available benchmark coating material, c-BN, shows a brittle nature with a G/B value of 1.02, which is an indication of extreme brittleness.[4] Despite the fact that Ti_2BC, Zr_2BC, and Hf_2BC are brittle, their G/B values are remarkably similar to those of other known coating materials.[2–5,7] A combination of high hardness and ductility is very attractive for engineering applications and in this respect W_2BC has significant potential in industrial sector.

3.4.2 Elastic anisotropy. The study of elastic anisotropy is important from the standpoint of applications like structural phase change and dislocation dynamics, among others. Furthermore, anisotropic behavior has recently been found to affect a variety of processes, including mechanical property changes, quantum dot alignment, microscale cracking in solids, and plastic deformation in materials.[35,38,39] As a result, quantifying elastic anisotropy for solids is critical prior to designing possible applications. Currently, there are varieties of indicators for determining the degree of anisotropy. For example, shear anisotropy factors, directional bulk modulus, anisotropy factors in compressibility and shear moduli, universal anisotropy index and so on are widely used.[18,35,40]

The elastic moduli and elastic stiffness constants of A_2BC (A = Ti, Zr, Hf, and W) compounds are used to calculate the anisotropy indicators to evaluate the degree of anisotropy. The related theory and formulae can be found elsewhere.[1,33] All results are summarized in Table S3.† It can be seen in the Table S3† that the values of the shear anisotropy factors A_i ($i = 1$, 2 and 3) for the crystal planes (100), (010), and (001), respectively, are off from the unity. This shows that the compounds under study have anisotropic character. The values of bulk modulus B_a, B_b,

Table 1 The calculated bulk modulus (B), shear modulus(G), Young's modulus (Y) (all in GPa), Pugh ratio (G/B), and Poisson ratio (ν) for A_2BC (A = Ti, Zr, Hf and W) compounds. The data for some other metallic boro-carbides and well known ceramic materials for surface coating applications (TiN, TiAlN, $Ti_{0.5}Al_{0.5}N$, $Ti_{0.25}Al_{0.75}N$, $Cr_{0.5}Al_{0.5}N$ and c-BN) are tabulated for comparison

Compound	B	G	Y	G/B	ν	Ref.
Ti_2BC	214	163	390	0.76	0.20	This
	208	158	378	0.76		3
Zr_2BC	193	136	330	0.70	0.22	This
	187	128	312	0.68		3
Hf_2BC	218	153	372	0.70	0.22	This
	207	150	362	0.72		3
W_2BC	353	188	479	0.53	0.27	This
	350	184	468	0.52		3
V_2BC	254	177	431	0.69	0.22	1
	260	178	435	0.68		3
Nb_2BC	263	169	418	0.64	0.23	1
	259	163	404	0.63		3
Mo_2BC	317	187	469	0.59	0.25	1
	324	187	470	0.58	0.26	4
	313	181	455	0.58		3
Ta_2BC	275	165	412	0.60	0.25	1
	286	168	421	0.59		3
TiN	295	213	514	0.72	0.22	5
TiAlN	257	178	434	0.69	0.22	5
$Ti_{0.5}Al_{0.5}N$	280	210	504[a]	0.75	0.20[a]	6
$Ti_{0.25}Al_{0.75}N$	178	123	300[a]	0.69	0.22[a]	4
$Cr_{0.5}Al_{0.5}N$	250	150[a]	375	0.60[a]	0.25	7
c-BN	376	382	856	1.01	0.12	4

[a] Calculated from the elastic constants.

and B_c (all in GPa) along the a, b, and c axes, respectively, show that the degree of axial bulk modulus follows the following sequence: $B_c > B_a > B_b$. Additionally, the percentage (%) of elastic anisotropy in compressibility (A_B) and shear (A_G) for the orthorhombic crystal structure can also be estimated using the following formulas: $A_B = \frac{B_V - B_R}{B_V + B_R} \times 100\%$, $A_G = \frac{G_V - G_R}{G_V + G_R} \times 100\%$. Among various anisotropy performance indicators, the universal anisotropy index (A^U) is the most versatile and acceptable indicator, which was developed by Ranganathan *et al.*[44] as $A^U = 5\frac{G_V}{G_R} + \frac{B_V}{B_R} - 6 \geq 0$, which may be used to all crystal symmetries to express crystal anisotropy as well. Here the subscripts, V stands for Voigt and R indicates Reuss bounds. According to the results of A_B, A_G and A^U, it can be concluded that the A_2BC (A = Ti, Zr, Hf, and W) compounds are elastically anisotropic. The anisotropies in elastic stiffness constants as well as elastic moduli are primarily caused by the anisotropic character of chemical bonds along different crystallographic axes.

3.4.3 Mulliken population, hardness and fracture toughness. According to the Table S4†, the elements B/C and Ti/Zr/Hf/W contain a negative and a positive charge, respectively. In compound, Ti_2BC, the electron from Ti is transferred to B (0.63) and C (0.72). The rest of the compounds (Zr_2BC, Hf_2BC, and W_2BC) have a similar charge transfer mechanisms, as shown in Table S4†. The values obtained from the bond overlap population analysis show that the bond strength of Ti/Zr/Hf/W–C is higher than those of Ti/Zr/Hf/W–B. In particular, the C–W bond belongs to the covalent bond and shows the highest bond strength than the other C–Ti/Zr/Hf bonds. In case of the Ti_2BC compound, the B–B bond is the strongest among the three remaining compounds. These results also agree with the findings of the EDD mapping images.

The resistance of a solid material to localized plastic deformation is measured by its hardness. The hardness of the material is important to understand the behavior in their practical applications. There are several methods to measure the hardness experimentally. For instance, the most popular methods are Brinell hardness, Rockwell hardness, Knoop hardness, and Vickers hardness.[41] The theoretical calculation of the hardness is not easy, rather complex. There are various proposed schemes to theoretically calculate the hardness as a function of bulk modulus and shear modulus. The formulae by X. Chen *et al.*,[42] Y. Tian *et al.*[43] and D. M. Teter[44] are based on either G or both G and B while N. Miao *et al.*[45] and E. Mazhnik *et al.*[41] formulae are mainly dependent on the Young's modulus and Poisson's ratio. These formulas are as follows:

$$(H_V)_{Chen} = 2[(G/B)^2 G]^{0.585} - 3 \quad (1)$$

$$(H_V)_{Tian} = 0.92(G/B)^{1.137} G^{0.708} \quad (2)$$

$$(H_V)_{Teter} = 0.151G \quad (3)$$

$$(H_V)_{Miao} = (1 - 2\nu)Y/6(1 + \nu) \quad (4)$$

$$(H_V)_{Mazhnik} = \gamma_0 \chi(\nu) Y \quad (5)$$

In eqn (5), $\chi(\nu)$ is a function of Poisson's ratio and can be written as:

$$\chi(\nu) = \frac{1 - 8.5\nu + 19.5\nu^2}{1 - 7.5\nu + 12.2\nu^2 + 19.6\nu^3}$$

where γ_0 is a constant with a value of 0.096 and has no dimension.

It can be seen from Table 2, that according to Chen and Tian formulae, the highest hardness value was obtained for Ti_2BC and the lowest value for the W_2BC compound. The intermediate values were obtained for the Zr_2BC and Hf_2BC compounds. On the other hand, using the Teter formula, the highest value (28.32 GPa) was for the W_2BC compound and the lowest value (20.53 GPa) was for the Zr_2BC compound. Based on these results, it is very difficult to predict the actual hardness of these compounds. It is reported that hardness differs from the elastic moduli of materials. The B and G cannot predict the hardness of some class of materials with high level of accuracy especially the materials having very low or negative value of Poisson's ratio (ν). Further details on this matter can be found in ref. 41. The hardness values of all the compounds under study obtained using the formula by N. Miao *et al.*[45] are much higher but follow almost the similar tendency of those found by using the Chen and Tian formulae.[42,43] Comparatively the most popular and acceptable method at present, is developed by E. Mazhnik *et al.*[41] This approach employs the Young moduli (Y) and Poisson's ratio (ν) to predict hardness. To calculate the hardness, the choice of Y and ν is reasonable because the B and G correlate highly with each other.[41] As indicated from the Table 2 that the hardnesses values due to the Mazhnik method are in the following order: W_2BC > Ti_2BC > Hf_2BC > Zr_2BC. It's worth noting that, with the exception of Hf_2BC, the results of electron density difference and Mulliken population analysis are quite similar with the order of hardness given above [see Section 3.2]. The Vickers hardness, which is a prominent theoretical approach to calculating intrinsic hardness was introduced by F. Gao[46] and H. Gou *et al.*[47] The computed Vickers hardness is mostly dependent on the Mulliken overlap population, which quantifies the degree of covalency of the bond and thus determines individual bonding strength. Again the strength of the bond is determined by the mean value of overlap populations per unit volume. However, the intrinsic hardness of a metallic material can be calculated by the following equation:[27,47]

Table 2 Calculated hardness (GPa) based on elastic moduli and Poisson's ratio for A_2BC (A = Ti, Zr, Hf and W) compounds

Compound	$(H_V)_{Chen}$	$(H_V)_{Tian}$	$(H_V)_{Teter}$	$(H_V)_{Miao}$	$(H_V)_{Mazhnik}$
Ti_2BC	25.63	24.86	24.61	33.00	21.23
Zr_2BC	20.51	20.02	20.53	25.86	16.05
Hf_2BC	22.07	21.66	23.10	29.00	17.99
W_2BC	17.47	18.31	28.38	28.34	23.49

$$H_V = \left[\prod^{\mu} \left\{ 740\left(P^{\mu} - P^{\mu'}\right)\left(v_b^{\mu}\right)^{-5/3} \right\}^{n^{\mu}} \right]^{1/\sum n^{\mu}} \quad (6)$$

where P^{μ} is the Mulliken population of the μ-type bond, $P^{\mu\prime} = n_{free}/V$, is the metallic population, and v_b^{μ} is the bond volume of μ-type bond. The number of free electrons, n_{free} is evaluated by $n_{free} = \int_{E_p}^{E_F} N(E)\mathrm{d}E$ where $N(E)$ is the density of state value at an energy E, E_p is the energy position of the pseudogap which is situated at the left of Fermi energy (E_F). Above E_p the nature of electrons should be delocalized. In the present study, as shown in Table 3, the value of Vickers hardness (in GPa) for A_2BC (A = Ti, Zr, Hf and W) compounds are 28.20, 23.12, 12.44 and 35.70, respectively. It is noticed here that the hardness values have increased with the sequence of A-element in A_2BC compound from Hf to Zr to Ti to W. The hardness value of W_2BC compares well with some well known compounds such as SiC, SiO_2, B_6O, B_6S and B_6Se.[18,21,41] The high valence electron concentration could be the possible reason of the highest value of Vickers hardness of the W_2BC compound.[3] It should be noted here that the shear elastic constant (C_{44}) and elastic moduli (B, G and Y) were also the highest for this particular compound. Moreover, the results of hardness are also compatible with the findings of electron density difference and Mulliken population analysis. Despite these predictions implying high hardness, the W_2BC compound should not be considered as a superhard (H_v > 40 GPa) material,[41,48] but at least, could be a member of the hard family. In summary, the hardness values of all the compounds under consideration varied since the hardness formulae (Chen, Tian, Teter, Mazhnik and Miao) have different functional forms and put emphasis on different elastic moduli. On the other hand, the Vickers hardness calculation depends on individual bond strength. For example, the elastic modulus (shear modulus) values of B_6O and TiN are almost the same, but the Vickers hardness (H_v) (experimental) of B_6O (38 GPa) is more than two times than that (17.6 GPa) of TiN. Again, the H_v (experimental) value for the OsB_2 compound is 29.4 GPa, while the hardness using Chen's formula is 17.8 GPa.[41] Therefore, our hardness results require experimental verification for further confirmation. Roughly speaking, theoretical analyses under different schemes predict W_2BC as the hardest among all the A_2BC (A = Ti, Zr, Hf and W) ternaries considered herein.

The crack formation, especially in metals and ceramic materials is one of the biggest problems of the surface hard coatings on heavy-duty tools. Fracture toughness, K_{IC} is a parameter, which can evaluate the resistance of a material to crack/fracture initiation. The formula for K_{IC} of a material is as follows:[41]

$$K_{IC} = \alpha_0^{-1/2} V_0^{1/6} [\xi(\nu) Y]^{3/2} \quad (7)$$

where V_0 = volume per atom; α_0 = 8840 GPa for covalent and ionic crystals; $\xi(\nu)$ is a dimensionless parameter and a function of Poisson's ratio (ν), which can be found from- $\xi(\nu) = \frac{1 - 13.7\nu + 48.6\nu^2}{1 - 15.2\nu + 70.2\nu^2 - 81.5\nu^3}$

As presented in Table 3, the values of K_{IC} of the A_2BC (M = Ti, Zr, Hf and W) compounds are 2.81, 2.38, 2.85 and 4.96 $MPam^{1/2}$, respectively. It is found that the highest resistance to crack formation and propagation is offered by the W_2BC compound. The K_{IC} value of W_2BC is well matched with those of some of the commercialized compounds, namely, WC, BN, diamond, and

Table 3 Muliken bond overlap population of μ-type bond P^{μ}, bond length d^{μ} (Å), metallic population $P^{\mu\prime}$, bond volume $v_b{}^{\mu}$ (Å^3), Vickers hardness of μ-type bond $H_V{}^{\mu}$ (GPa), Vickers hardness, H_V (GPa), fracture toughness, K_{IC} ($MPam^{1/2}$), and index of brittleness, B_i $(\mu m)^{-1/2}$ of A_2BC (A = Ti, Zr, Hf and W) compounds

Compound	Bond	d^{μ}	P^{μ}	$P^{\mu\prime}$	$v_b{}^{\mu}$	$H_V{}^{\mu}$	H_V	K_{IC}	H_V/K_{IC}
Ti_2BC	B–B	1.78777	1.47	0.0348	2.9369	175.5807			
	C–Ti(I)	2.07903	0.25		4.6190	12.3286			
	C–Ti(II)	2.10977	0.24		4.8269	10.9200	28.20	2.81	10.00
	C–Ti(III)	2.19435	1.51		5.43105	64.65076			
	B–Ti(I)	2.32277	0.89		6.4414	28.1776			
Zr_2BC	C–Zr(I)	2.29162	0.35	0.0262	5.98995	12.1076			
	C–Zr(II)	2.29402	0.30		6.0079	10.18093			
	C–Zr(III)	2.3656	1.42		6.5881	44.52817	23.12	2.38	9.71
	B–Zr(I)	2.52756	0.94		8.0360	20.95955			
	B–B	1.87731	1.42		3.29265	141.469			
Hf_2BC	C–Hf(I)	2.27847	0.41	0.0060	7.1606	11.212			
	C–Hf(II)	2.30038	0.48		10.2939	12.544			
	C–Hf(III)	2.36171	1.51		7.9744	34.94404	12.44	2.85	4.37
	B–Hf(II)	2.50748	1.14		9.5440	19.52519			
	B–Hf(III)	3.16178	0.21		19.1344	1.09774			
	B–B	1.90007	1.43		4.1526	98.1533			
W_2BC	B–B	1.82386	1.20	0.0176	2.4491	195.9051			
	C–W(I)	2.10329	0.14		3.7560	9.8833	35.70	4.96	7.19
	C–W(II)	2.16423	0.22		4.0921	14.1907			
	C–W(III)	2.19304	1.54		4.25773	100.1959			
	B–W(I)	2.31895	0.98		5.0942	46.9345			

Si_3N_4.[49,50]The hardness and fracture toughness ratio is called an index of brittleness (B_i) of a solid.[49] The B_i expresses the degree of damage tolerance. The lower value of B_i indicates higher damage tolerance of materials. In the present study, the value of B_i for A_2BC (A = Ti, Zr, Hf, and W) compounds are 10.00, 9.71, 4.37, and 7.19, respectively. It is seen that the Hf_2BC shows the highest damage tolerance among all the compounds under consideration. Noted here that the hardness value (H_v = 35.70 GPa) of W_2BC is much higher than that (H_v = 12.44 GPa) of Hf_2BC, even though it is somewhat less damage tolerant.

The machinability index is considered to evaluate the machinability of A_2BC (A = Ti, Zr, Hf and W) compounds. The machinability may differ depending on the cutting technique. The greater a material's machinability index value, the more machinable it is.[21] The value of machinability index (B/C_{44}) is 1.45, 1.59, 1.65, 1.91 for Ti_2BC, Zr_2BC, Hf_2BC and W_2BC respectively. As a result, it is obvious that the W_2BC compound is more machinable than the other compounds. High hardness together with high machinability once again makes W_2BC an attractive compound for machine tools applications.

3.5 Thermal properties

Thermal properties measure the response of a material to the applied heat. Study of thermal properties such as Debye temperature (Θ_D), thermal conductivity (K), specific heats (C_v, C_p), thermal expansion coefficient (α), and melting temperature (T_m) are essential to comprehend the temperature dependent behaviors of A_2BC (A = Ti, Zr, Hf and W) ternaries. For many high temperature device applications, thermal barrier coating (TBC) materials are an important requisite. A popular application of TBC is the coating on turbine blades in gas-turbine engines which facilitates its use at elevated operating temperature, resulting in the high efficiency of the engines.[35]

In the sub-sections to follow, we will study the various thermal properties such as Debye temperature, lattice thermal conductivity, minimum thermal conductivity, specific heat and thermal expansion coefficient of A_2BC (A = Ti, Zr, Hf and W) in detail.

3.5.1 Debye temperature and thermal conductivity. Debye temperature, Θ_D measures the highest vibrational frequency of a crystalline material. The Θ_D can be calculated from the sound velocity which depends on the polycrystalline elastic moduli. Related formula and theory can be found in the previous reports.[21,27,35,51–53] It is seen from Table 4, that the highest Θ_D is found for Ti_2BC and lowest value is for Hf_2BC. The Θ_D is largely dependent on the mean sound velocity, which is increased with the increase of v_m except for W_2BC. It is also seen that longitudinal sound velocity is larger than transverse sound velocity in case of all the studied materials.

The thermal conductivity of a material plays an important role to design power-dissipating device and/or thermoelectric device. A high value of thermal conductivity of a material is used as heat sink while its low value is helpful to increase the figure of merit of a thermoelectric device. The lattice thermal conductivity (K_{ph}) of a solid originates from the conduction of heat due to the lattice vibrations. The total thermal conductivity is a combination of lattice thermal conductivity and electronic thermal conductivity. The thermal conductivity of a material plays an important role to design many useful devices like power-dissipating device, thermoelectric device, thermal barrier coating (TBC) materials *etc.* As an example, a high value of thermal conductivity of a material is used as heat sink while its low value is helpful to increase the figure of merit of a thermoelectric device and TBC materials.[21] Here, we will discuss only the lattice thermal conductivity (k_{ph}). In all materials, the lattice thermal conductivity dominates at high temperatures. The k_{ph} of a material is measured by the heat conduction due to lattice vibration. Slack derived an empirical formula to estimate the k_{ph} theoretically as follows:[54]

$$K_{ph} = A(\gamma)\frac{M_{av}\Theta_D{}^3\delta}{\gamma^2 n^{2/3}\,T}$$

$$\gamma = \frac{3(1+\upsilon)}{2(2-3\upsilon)}$$

where, γ is the acoustic Grüneisen parameter which measures the degree of anharmonicity of phonons. A material with small value of Grüneisen parameter indicates low anharmonicity of phonons which results in high thermal conductivity. The coefficient $A(\gamma)$ is evaluated by the following equation:

Table 4 Calculated crystal density, longitudinal, transverse and average sound velocities (v_l, v_t, and v_m), Debye temperature, Θ_D, minimum thermal conductivity, K_{min}, lattice thermal conductivity (k_{ph}) and Grüneisen parameter, γ for A_2BC (M = Ti, Zr, Hf and W) compounds

Compounds	ρ (gm cm^{-3})	v_l (m s^{-1})	v_t (m s^{-1})	v_m (m s^{-1})	Θ_D (K)	K_{min} (W mK^{-1})	$k_{ph}{}^a$ (W mK^{-1})	γ	Ref.
Ti_2BC	4.66	9616	5915	6527	886	1.87	48.30	1.29	This
Zr_2BC	6.33	7692	4637	5127	642	1.25	30.23	1.37	This
Hf_2BC	11.85	5964	3590	3971	499	0.97	26.17	1.36	This
W_2BC	15.51	6240	3482	3877	528	1.12	20.79	1.60	This
V_2BC	05.63	9331	5608	6202	881	1.95	—	1.36	1
Nb_2BC	07.50	8068	4746	5260	693	1.42	—	1.40	1
Mo_2BC	08.60	8116	4664	5180	707	1.50	—	1.50	1
Ta_2BC	13.33	6094	3518	3906	508	1.03	—	1.51	1

[a] Calculated at 300 K.

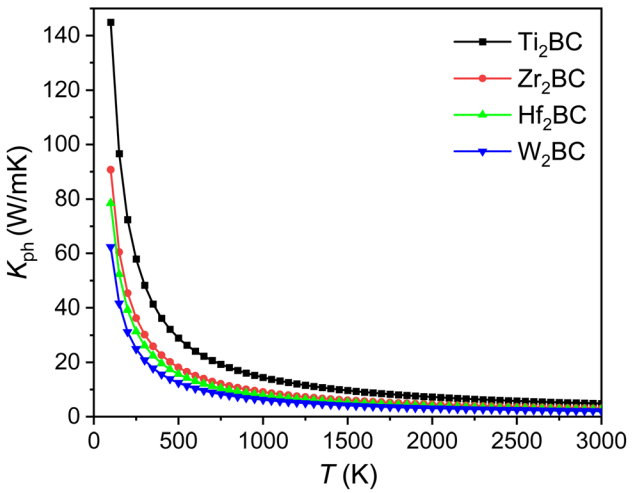

Fig. 6 The lattice thermal conductivity (K_{ph}) as a function of temperature of the A_2BC (A = Ti, Zr, Hf, and W) compounds.

$$A(\gamma) = \frac{4.85628 \times 10^7}{2\left(1 - \frac{0.514}{\gamma} + \frac{0.228}{\gamma^2}\right)}$$

The k_{ph} for the A_2BC (A = Ti, Zr, Hf and W) compounds are a decreasing function of temperature given by: 14 491.33/T, 9071.07/T, 7851.76/T and 6237.72/T, respectively. The value of k_{ph} is almost constant after ~1000 K as shown in Fig. 6. The lattice thermal conductivity, k_{ph} at temperature 300 K and Grüneisen parameter, γ are tabulated in Table 4. At room temperature (300 K), the k_{ph} value (in W mK^{-1}) for the A_2BC (A = Ti, Zr, Hf and W) compounds follow the following order: 48.30 > 30.23 > 26.17 > 20.79. It is noted here that the compound, Ti_2BC contains the highest value of lattice thermal conductivity due to high value of Θ_D. This value is comparable with B_6X (X = S, Se), MAX phase compounds, bronze, brass and aluminum bronze, but is much lower than SiC, copper, diamond, aluminium nitride *etc.*[21,55–57] It is well known that high thermal conductivity materials can be used as heat sink materials in laptops or any other microelectronic devices as heat dissipating agency. The value of minimum thermal conductivity can be calculated based on the modified Clarke's model and the equation can be represented as follows:[58]

$$K_{min} = k_B v_m \left(\frac{M}{n\rho N_A}\right)^{-\frac{2}{3}}$$

The value of minimum thermal conductivity, K_{min} can be found in Table 4. It is found that the values of Θ_D and K_{min} for Hf_2BC and W_2BC are much lower and these values are comparable with well known commercialized TBC material, $Y_4Al_{12}O_9$ (K_{min} = 1.13 W mK^{-1}; Θ_D = 564 K).[59,60] The K_{min} (W mK^{-1}) value for Hf_2BC (0.97) and W_2BC (1.12) compounds are also comparable with some other compounds such as metallic borocarbides, Ta_2BC (1.03),[1] MAB phase Hf_3PB_4 (1.14),[31] MAX phase Ti_2SnC (0.99)[61] and so on. The melting temperatures (T_m in K) for A_2BC (A = Ti, Zr, Hf and W) compounds are calculated using the formula in ref. 31, 40 and 62 and are found to be 2073 K, 1884 K, 2054 K and 2615 K, respectively. It is found that the maximum T_m value is attained for W_2BC owing to the high hardness and bond strength of this compound.

3.5.2 Heat capacities and thermal expansion coefficients. The Debye heat capacity at constant volume (C_v) of the compounds can be estimated based on the quasi-harmonic Debye model:[63–66]

$$C_v = 9nN_A k_B \left(\frac{T}{\Theta_D}\right)^3 \int_0^{x_D} dx \frac{x^4 e^x}{(e^x - 1)^2}$$

where, $x_D = \frac{\Theta_D}{T}$; and n is the number of atoms per formula unit, N_A is the Avogadro's number and k_B is the Boltzmann constant. The linear thermal expansion coefficient (α) and specific heat at constant pressure (C_p) can be determined from the following equations:[21,35]

$$\alpha = \frac{\gamma C_v}{3B_T v_m} \text{ and } C_p = C_v(1 + \alpha\gamma T)$$

where, B_T is the isothermal bulk modulus, v_m is the molar volume, and γ is the Grüneisen parameter.

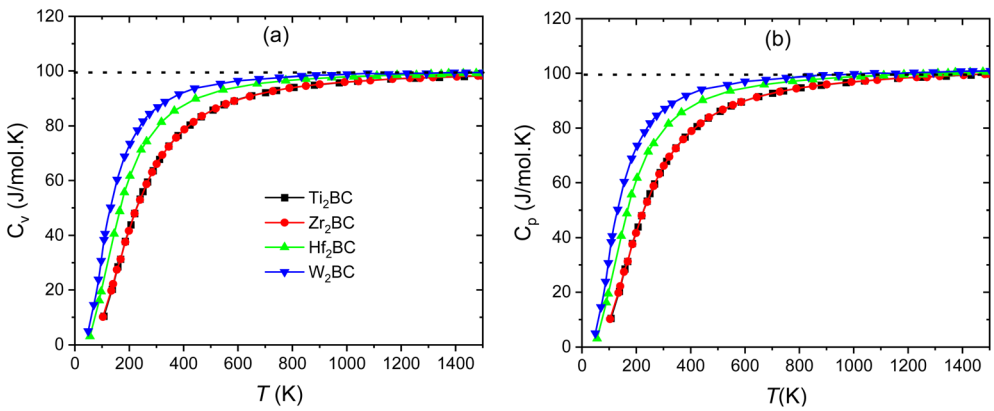

Fig. 7 Specific heats (a) C_v, and (b) C_p of the A_2BC (A = Ti, Zr, Hf and W) compounds as a function of temperature. The dashed line marks the classical Dulong–Petit limit.

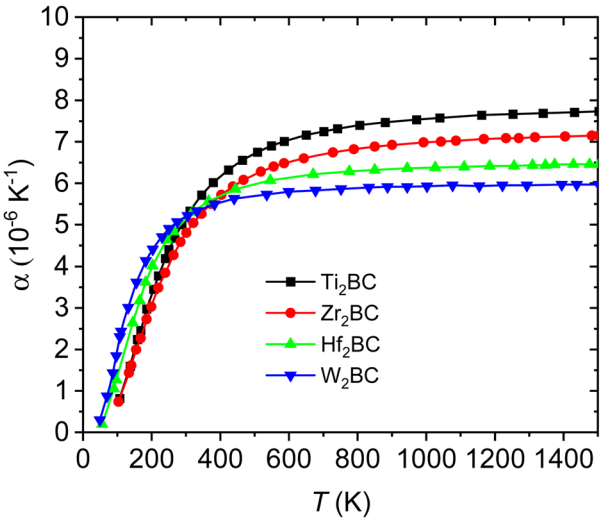

Fig. 8 Linear thermal expansion coefficient for the A_2BC (A = Ti, Zr, Hf and W) compounds as a function of temperature.

Fig. 7(a–b) and Fig. 8 display the temperature dependence of Debye specific heats, C_v, C_p and α for A_2BC (A = Ti, Zr, Hf and W) compounds in the temperature range of 0–1500 K where the quasi-harmonic Debye model is expected to be valid.

The phononic thermal softening occurs with increasing temperature. As a result the heat capacity also increases with increasing temperature. Both heat capacities and linear thermal expansion coefficient have an increasing tendency with temperature. The temperature dependences are steep at low temperature region, indicating to an increased ability of the lattice waves to enhance their average energy with ascending temperature. At low temperature, the relationship between heat capacities and temperature meets the Debye-T^3 power-law.[67] It is noticed that at high temperature the heat capacities approach the Dulong–Petit (DP) ($3nN_Ak_B$) limit.[68] The value of C_v (J mol^{-1} K^{-1}) at room temperature (300 K) is found to be different for different compounds and followed the sequence: W_2BC (86.9) > Hf_2BC (81.4) > Zr_2BC (66.08) > Ti_2BC (65.7).

The thermal expansion coefficient (α) of solids can be estimated from the difference between C_p and C_v. Temperature dependences of α are illustrated in Fig. 8 for the A_2BC (A = Ti, Zr, Hf and W) compounds. It is found that like C_p and C_v, the values of α also increase rapidly up to the room temperature (300 K) and then gradually goes to a constant value at higher temperatures. At room temperature, the values of α are as follows: Ti_2BC (5.33×10^{-6} K^{-1}), Zr_2BC (4.81×10^{-6} K^{-1}), Hf_2BC (5.10×10^{-6} K^{-1}) and W_2BC (5.21×10^{-6} K^{-1}).

To summarize, to predict a compound as an efficient TBC material, the following characteristics should be considered. The solid should have damage tolerant behavior, low value of K_{min}, comparatively high T_m, comparatively low Θ_D and low thermal expansion coefficient (α). In our case, we have found favorable data sets for Hf_2BC and W_2BC compounds. So we can suggest that these two compounds can be used as promising TBC materials. The high value of lattice thermal conductivity (k_{ph}), K_{min}, α and Θ_D for the Ti_2BC compound, on the other hand, give strong indication of its use as a heat sink material.

4. Conclusions

The first-principles approach has been adopted to perform a comprehensive theoretical study on ternary metallic borocarbides A_2BC (A = Ti, Zr, Hf, and W) using the state-of-the-art density functional theory. The study focuses on these compounds' physical aspects such as structural, electronic, optical, mechanical, and thermal properties. Characterizing parameters for orthorhombic unit cells, such as lattice parameters and volume, are clearly justified in the light of prior research. Because there is no band gap between the valence and conduction bands, all of the compounds tested are metallic in nature. The total density of states at the Fermi level of A_2BC (A = Ti, Zr, Hf, and W) compounds are 5.80, 5.85, 4.76, and 5.41 states per eV, respectively. Relatively high values of TDOS at the Fermi level result from some flat bands crossing this particular energy. The compounds under study are mechanically stable. These compounds are also predicted to be anisotropic in nature. The compound W_2BC shows ductile deformation, but the deformation characteristic is brittle for the other three compounds (Ti_2BC, Zr_2BC, and Hf_2BC). The hardness of the materials is evaluated using the approach of Chen, Tian, Teter, Mazhnik, Miao, and Vickers hardness. It is found that the W_2BC compound has the highest Vickers hardness rating among all the compounds under investigation. The predicted Vickers hardness value is increased for the metallic element in the following sequence: $Hf_2BC < Zr_2BC < Ti_2BC < W_2BC$, which also followed the shear elastic constant, C_{44}, and elastic moduli (B, G, and Y) except for Hf_2BC. The value of the machinability index is 1.45, 1.59, 1.65, and 1.91 for Ti_2BC, Zr_2BC, Hf_2BC, and W_2BC, respectively, indicating that W_2BC compounds are more machinable than the other compounds. Various optical properties (such as dielectric function, refractive index, absorption coefficient, photoconductivity, reflectivity and loss function) are computed based on Kramer–Kronig relation and discussed in detail. Reflectivity spectra show for Ti_2BC (>53%) and W_2BC (>45%) in the IR, visible, and UV regions (<10 eV, at least), indicating the possible use as of these as coating materials to avoid solar heating. The study of various thermal properties such as Debye temperature, melting temperature, thermal conductivity, and thermal expansion coefficient suggest that Ti_2BC could be used as heat sink material, whereas Hf_2BC and W_2BC possess significant promise as TBC materials.

Data availability

The datasets generated during the current study are available from the corresponding authors on a reasonable request.

Conflicts of interest

The authors declare that they have no known competing financial interests or personal relationships that could have appeared to influence the work reported in this paper.

Acknowledgements

This work was carried out with the aid of a grant (No. 21-378 RG/PHYS/AS_G-FR3240319526) from UNESCO-TWAS and the Swedish International Development Cooperation Agency (Sida). The views expressed herein do not necessarily represent those of UNESCO-TWAS, Sida or its Board of Governors. Authors are also grateful to the Department of Physics, Chittagong University of Engineering & Technology (CUET), Chattogram-4349, Bangladesh, for providing the computing facilities for this work.

References

1 P. Barua, M. M. Hossain, M. A. Ali, M. M. Uddin, S. H. Naqib and A. K. M. A. Islam, *J. Alloys Compd.*, 2019, **770**, 523–534.
2 S.-Y. Yoon, J.-K. Kim and K. H. Kim, *Surf. Coat. Technol.*, 2002, **161**, 237–242.
3 H. Bolvardi, J. Emmerlich, M. to Baben, D. Music, J. von Appen, R. Dronskowski and J. M. Schneider, *J. Phys.: Condens. Matter*, 2012, **25**, 045501.
4 J. Emmerlich, D. Music, M. Braun, P. Fayek, F. Munnik and J. M. Schneider, *J. Phys. D: Appl. Phys.*, 2009, **42**, 185406.
5 K. Chen, L. R. Zhao, J. Rodgers and J. S. Tse, *J. Phys. D: Appl. Phys.*, 2003, **36**, 2725–2729.
6 P. H. Mayrhofer, D. Music and J. M. Schneider, *J. Appl. Phys.*, 2006, **100**, 094906.
7 P. H. Mayrhofer, D. Music, Th. Reeswinkel, H.-G. Fuß and J. M. Schneider, *Acta Mater.*, 2008, **56**, 2469–2475.
8 S. F. Pugh, *London, Edinburgh Dublin Philos. Mag. J. Sci.*, 1954, **45**, 823–843.
9 J.-O. Bovin, M. O'Keeffe and L. Stenberg, *J. Solid State Chem.*, 1977, **22**, 221–231.
10 P. Lejay, B. Chevalier, J. Etourneau and P. Hagenmuller, *J. Less-Common Met.*, 1981, **82**, 193–200.
11 B. Bressel, B. Chevalier, J. Etourneau and P. Hagenmuller, *J. Cryst. Growth*, 1979, **47**, 429–433.
12 P. H. Mayrhofer, D. Music, Th. Reeswinkel, H.-G. Fuß and J. M. Schneider, *Acta Mater.*, 2008, **56**, 2469–2475.
13 W. Kohn and L. J. Sham, *Phys. Rev.*, 1965, **140**, A1133–A1138.
14 S. J. Clark, M. D. Segall, C. J. Pickard, P. J. Hasnip, M. I. J. Probert, K. Refson and M. C. Payne, *Z. Kristallogr. - Cryst. Mater.*, 2005, **220**, 567–570.
15 M. D. Segall, P. J. D. Lindan, M. J. Probert, C. J. Pickard, P. J. Hasnip, S. J. Clark and M. C. Payne, *J. Phys.: Condens. Matter*, 2002, **14**, 2717–2744.
16 J. P. Perdew, K. Burke and M. Ernzerhof, *Phys. Rev. Lett.*, 1996, **77**, 3865–3868.
17 H. J. Monkhorst and J. D. Pack, *Phys. Rev. B: Condens. Matter Mater. Phys.*, 1976, **13**, 5188–5192.
18 Md. M. Hossain, Md. A. Ali, Md. M. Uddin, S. H. Naqib and A. K. M. A. Islam, *ACS Omega*, 2021, **6**, 33899–33913.
19 M. A. Hadi, R. V. Vovk and A. Chroneos, *J. Mater. Sci.: Mater. Electron.*, 2016, **27**, 11925–11933.
20 M. M. Hossain, M. A. Hossain, S. A. Moon, M. A. Ali, M. M. Uddin, S. H. Naqib, A. K. M. A. Islam, M. Nagao, S. Watauchi and I. Tanaka, *J. Mater. Sci.: Mater. Electron.*, 2021, **32**, 3878–3893.
21 M. M. Hossain, M. A. Ali, M. M. Uddin, A. K. M. A. Islam and S. H. Naqib, *J. Appl. Phys.*, 2021, **129**, 175109.
22 *What are High Refractive Index Materials?*, **https://avantama.com/what-are-high-refractive-index-materials/**, accessed May 27, 2022.
23 Z. Abbas, K. Fatima, M. Abubakr, I. Gorczyca, T. Alshahrani, S. Muhammad and A. G. Al-Sehemi, *Optik*, 2022, **250**, 168289.
24 K. Fatima, Z. Abbas, A. Naz, T. Alshahrani, Y. Chaib, S. H. A. Jaffery, S. Muhammad, S. Hussain, J. Jung and H. Algarni, *J. Solid State Chem.*, 2022, **313**, 123305.
25 M. S. Hossain, M. A. Ali, M. M. Hossain and M. M. Uddin, *Mater. Today Commun.*, 2021, **27**, 102411.
26 M. A. Ali, M. M. Hossain, M. M. Uddin, M. A. Hossain, A. K. M. A. Islam and S. H. Naqib, *J. Mater. Res. Technol.*, 2021, **11**, 1000–1018.
27 A. Chowdhury, M. A. Ali, M. M. Hossain, M. M. Uddin, S. H. Naqib and A. K. M. A. Islam, *Phys. Status Solidi B*, 2018, **255**, 1700235.
28 F. Sultana, M. M. Uddin, M. A. Ali, M. M. Hossain, S. H. Naqib and A. K. M. A. Islam, *Results Phys.*, 2018, **11**, 869–876.
29 Z. Abbas, K. Fatima, S. H. A. Jaffery, A. Ali, H. H. Raza, S. Muhammad, H. Algarni, S. Hussain and J. Jung, *J. Comput. Sci.*, 2022, **63**, 101791.
30 S. Li, R. Ahuja, M. W. Barsoum, P. Jena and B. Johansson, *Appl. Phys. Lett.*, 2008, **92**, 221907.
31 M. A. Ali, M. M. Hossain, A. K. M. A. Islam and S. H. Naqib, *J. Alloys Compd.*, 2021, **857**, 158264.
32 F. Mouhat and F.-X. Coudert, *Phys. Rev. B: Condens. Matter Mater. Phys.*, 2014, **90**, 224104.
33 M. A. Ali, M. A. Hadi, M. M. Hossain, S. H. Naqib and A. K. M. A. Islam, *Phys. Status Solidi B*, 2017, **254**, 1700010.
34 S.-H. Jhi, J. Ihm, S. G. Louie and M. L. Cohen, *Nature*, 1999, **399**, 132–134.
35 M. M. Hossain, M. A. Ali, M. M. Uddin, M. A. Hossain, M. Rasadujjaman, S. H. Naqib, M. Nagao, S. Watauchi and I. Tanaka, *Mater. Today Commun.*, 2021, **26**, 101988.
36 W. Voigt, *Lehrbuch Der Kristallphysik*, Vieweg + Teubner Verlag, Wiesbaden, 1966.
37 R. Hill, *Proc. Phys. Soc., London, Sect. A*, 1952, **65**, 349–354.
38 C. M. Kube, *AIP Adv.*, 2016, **6**, 095209.
39 D. H. Chung and W. R. Buessem, *J. Appl. Phys.*, 1967, **38**, 2010–2012.
40 Md. M. Rahaman, M. H. K. Rubel, Md. A. Rashid, M. A. Alam, K. M. Hossain, Md. I. Hossain, A. A. Khatun, Md. M. Hossain, A. K. M. A. Islam, S. Kojima and N. Kumada, *J. Mater. Res. Technol.*, 2019, **8**, 3783–3794.
41 E. Mazhnik and A. R. Oganov, *J. Appl. Phys.*, 2019, **126**, 125109.
42 X.-Q. Chen, H. Niu, D. Li and Y. Li, *Intermetallics*, 2011, **19**, 1275–1281.
43 Y. Tian, B. Xu and Z. Zhao, *Int. J. Refract. Hard Met.*, 2012, **33**, 93–106.
44 D. M. Teter, *MRS Bull.*, 1998, **23**, 22–27.

45 N. Miao, B. Sa, J. Zhou and Z. Sun, *Comput. Mater. Sci.*, 2011, **50**, 1559–1566.
46 F. Gao, J. He, E. Wu, S. Liu, D. Yu, D. Li, S. Zhang and Y. Tian, *Phys. Rev. Lett.*, 2003, **91**, 015502.
47 H. Gou, L. Hou, J. Zhang and F. Gao, *Appl. Phys. Lett.*, 2008, **92**, 241901.
48 R. A. Andrievski, *Int. J. Refract. Hard Met.*, 2001, **19**, 447–452.
49 B. R. Lawn and D. B. Marshall, *J. Am. Ceram. Soc.*, 1979, **62**, 347–350.
50 H. Niu, S. Niu and A. R. Oganov, *J. Appl. Phys.*, 2019, **125**, 065105.
51 O. L. Anderson, *J. Phys. Chem. Solids*, 1963, **24**, 909–917.
52 A. J. Slifka, B. J. Filla, J. M. Phelps, G. Bancke and C. C. Berndt, *J. Therm. Spray Technol.*, 1998, **7**, 43–46.
53 M. S. Ali, A. K. M. A. Islam, M. M. Hossain and F. Parvin, *Phys. Rev. B: Condens. Matter Mater. Phys.*, 2012, **407**, 4221–4228.
54 G. A. Slack, *Phys. Solid State*, 1979, **34**, 1–71.
55 J. Haines, J. Léger and G. Bocquillon, *Annu. Rev. Mater. Res.*, 2001, **31**, 1–23.
56 E. Haque, *ACS Appl. Energy Mater.*, 2021, **4**, 1942–1953.
57 L.-F. Zhu, B. Grabowski and J. Neugebauer, *Phys. Rev. B: Condens. Matter Mater. Phys.*, 2017, **96**, 224202.
58 D. R. Clarke, *Surf. Coat. Technol.*, 2003, **163–164**, 67–74.
59 X. Zhan, Z. Li, B. Liu, J. Wang, Y. Zhou and Z. Hu, *J. Am. Ceram. Soc.*, 2012, **95**, 1429–1434.
60 Y. Zhou, H. Xiang, X. Lu, Z. Feng and Z. Li, *J. Adv. Ceram.*, 2015, **4**, 83–93.
61 M. A. Hadi, N. Kelaidis, S. H. Naqib, A. Chroneos and A. K. M. A. Islam, *J. Phys. Chem. Solids*, 2019, **129**, 162–171.
62 M. E. Fine, L. D. Brown and H. L. Marcus, *Scr. Mater.*, 1984, **18**, 951–956.
63 M. A. Blanco, E. Francisco and V. Luaña, *Comput. Phys. Commun.*, 2004, **158**, 57–72.
64 O. Delaire, A. F. May, M. A. McGuire, W. D. Porter, M. S. Lucas, M. B. Stone, D. L. Abernathy, V. A. Ravi, S. A. Firdosy and G. J. Snyder, *Phys. Rev. B: Condens. Matter Mater. Phys.*, 2009, **80**, 184302.
65 T. Plirdpring, K. Kurosaki, A. Kosuga, T. Day, S. Firdosy, V. Ravi, G. J. Snyder, A. Harnwunggmoung, T. Sugahara, Y. Ohishi, H. Muta and S. Yamanaka, *Adv. Mater.*, 2012, **24**, 3622–3626.
66 L. Xue, Y.-M. Ren, J.-R. He and S.-L. Xu, *Chin. Phys. B*, 2017, **26**, 067103.
67 P. Debye, *Ann. Phys.*, 1912, **344**, 789–839.
68 R. Fox, *Br. J. Hist. Sci.*, 1968, **4**, 1–22.